



Preliminary Study as Temperature Sensor of Nanosilica Based on Coastal and River Sand

Lalu Ahmad Didik Meiliyadi^{1,2*}, Muh. Wahyudi^{1,2}, Kurniawan Arizona^{1,2}

¹*Department of Physic Education, Faculty of Education and Teacher Training, Universitas Islam Negeri Mataram, Mataram, Indonesia*

²*Advance Science and Integration Research Group, Universitas Islam Negeri Mataram, Mataram, Indonesia*

*E-mail korespondensi: laludidik@uinma.ac.id

Article Info:

Sent:
[December 08, 2024](#)

Revision:
[January 23, 2025](#)

Accepted:
[January 23, 2025](#)

Keywords:

[Iron sand](#), [Magnetic mineral](#), [Nanosilica](#), [Sol gel](#), [Temperature sensor](#).

Abstract

The synthesis of nano-silica gel based on magnetic minerals from the coastal sand and river sand of Lombok Island has been carried out. The synthesis method used is sol-gel with HCl acid and NH₄OH base. The results showed that nano-silica based on coastal sand has a greater silica content than nanosilica based on river sand. The morphology of nanosilica based on coastal is granular with a smaller grain size of nanosilica based on coastal sand compared to nanosilica based on river sand. To a temperature sensor, nano-silica based on coastal sand has a larger coefficient when compared to nanosilica based on river sand. This indicates that nano-silica based on coastal sand has better physical properties as a temperature sensor than nanosilica based on river sand.

© 2024 State Islamic University of Mataram

INTRODUCTION

Indonesia is one of the largest producers of iron sand magnetic minerals in the world. This is because Indonesia is the country with the fourth longest coastline in the world. Apart from the coast, Indonesia also has rivers as a producer of iron sand magnetic minerals [1]. Iron sand magnetic minerals have mineral content that varies depending on the local source [2]. In general, iron sand magnetic minerals consist of Fe, Si, Ti, and Ni elements [3], [4].

One of the areas in Indonesia that contains iron sand is the island of Lombok [5]. The areas of Lombok Island that have a large enough iron sand magnetic mineral content are the Mataram area [1], Telindung [6] and Pringgabaya. In general, the most dominant magnetic mineral content found on Lombok Island is quartz sand (SiO₂).

Silica is one of the most widely used compounds in daily life such as raw materials for solar cells [7], oil purifiers [8], catalysts [9], [10], antimicrobial [11], filler [12], [13], [14] and sensor [15], [16], [17]. The application of nano-silica as a sensor is an interesting study because of its economical nature [18], [19].

Sensors are electronic devices used to detect physical and chemical quantities in the surrounding environment [20], [21]. One of the most important sensors in life is the temperature sensor [22], [23], [24]. In general, temperature sensors use CMOS (complementary metal oxide semiconductor) material based on silica (SiO₂) as the temperature field. Silica is a material that is widely contained in iron sand magnetic materials [25].

Previous research on the synthesis and utilization of nano silica based on magnetic minerals has been carried out. Ananda & Aini, (2021) successfully synthesized mesopore silica by using the sol gel method. Meiliyadi et al., (2023) synthesized nanosilica using the wet method and found that the nanosilica based on iron sand formed was influenced by the molarity of the NaOH solution used in the synthesis process. Bramantya et al., (2018) synthesized silica aerogel from sea sand as an oil spill absorbent and produced nano-silica absorbents that can absorb an average oil of 13.98 g per mass of silica aerogel.

However, the utilization of nano silica based on coastal sand and river sand as sensors has not been carried out. Nano silica is the basic material of CMOS which is a temperature sensor. Therefore, it is necessary to study and research the characteristics of nano silica based on river and coastal sand as temperature sensors.

EXPERIMENTAL METHOD

The synthesis method used in this study was the sol-gel [1]. In addition, the materials used are HCl with a concentration of 10 M Physical Analysis (99%). NH₄OH with a concentration of 9 M Physical Analysis (99%) and deionized water. Mineral magnetic river sand and coastal then dried in the sun for 2 days to dry. Mineral magnetic river sand and coastal are then separated from impurities using a permanent magnet. Furthermore, washing is done using distilled water 5 times and dried. After washing, the magnetic minerals of river sand and coastal sand are dried in an oven at 80 °C for 12 hours to remove the water content in them [28]. The flow chart of the synthesis of silica is shown in Figure 1. The synthesis metode as the previous study [1], [5].

Morphological characterization of nano-silica gel was carried out by using SEM and mineral content analysis by using EDX type Jeol 700. The measurement of nano silica characteristics as a temperature sensor is shown in Figure 2.

Measurement of nano-silica gel temperature sensor characteristics by using the circuit shown in Figure 2. The laser beam used has a wavelength of 250 nm. The light intensity used uses a lux meter type Benetech GM1010.

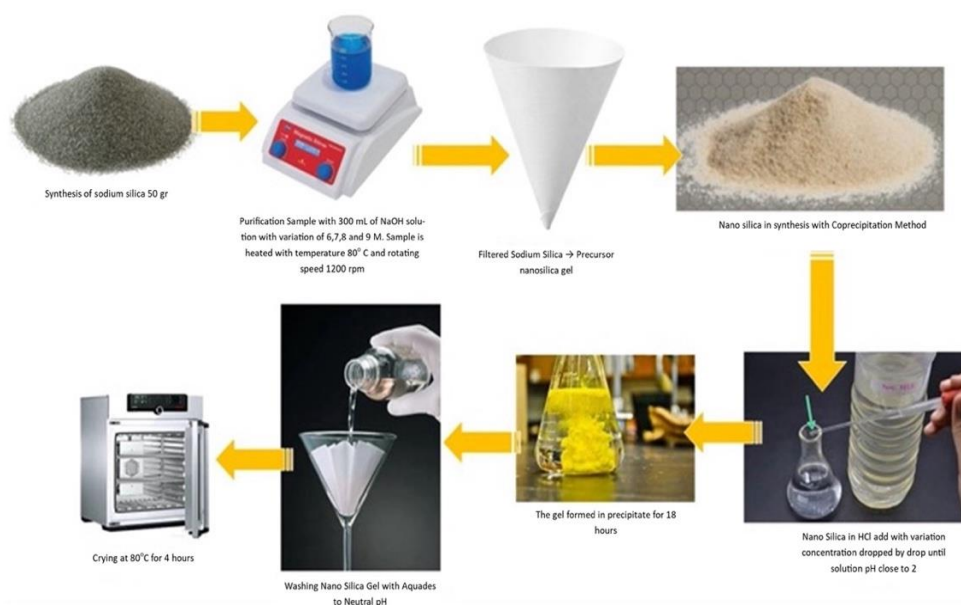


Figure 1. Flowchart of Nanosilica Synthesis Based on Coastal and River Sand

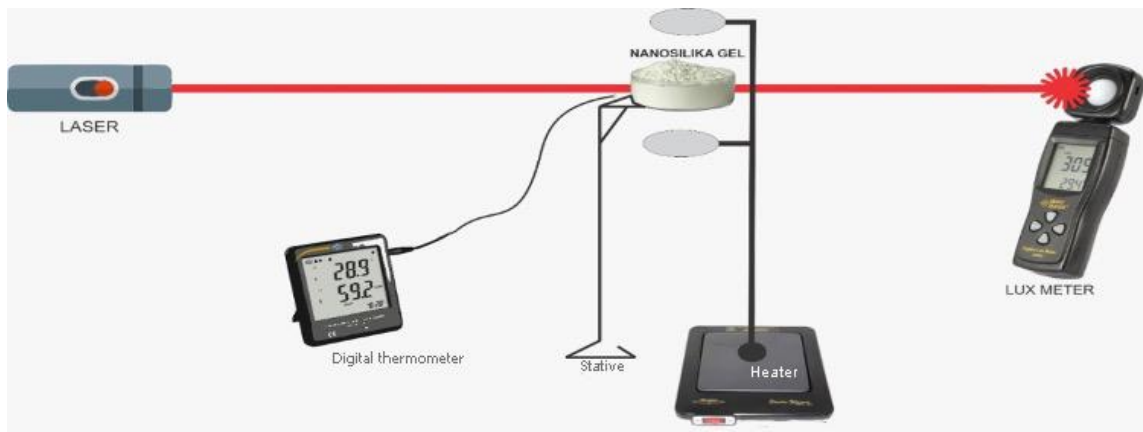
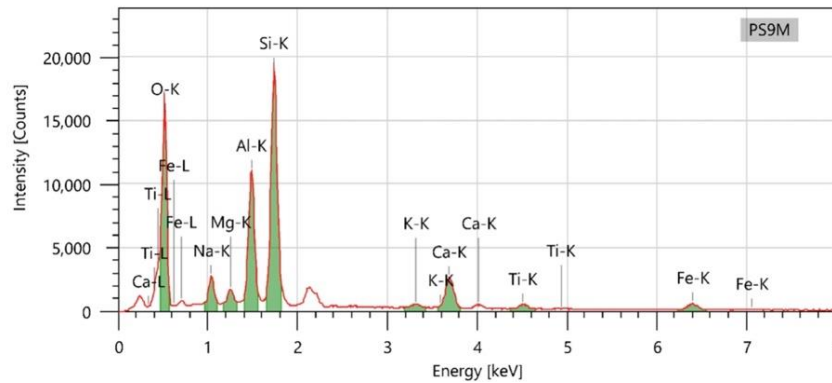


Figure 2. Schematic of Nanosilica Measurement as a Temperature Sensor

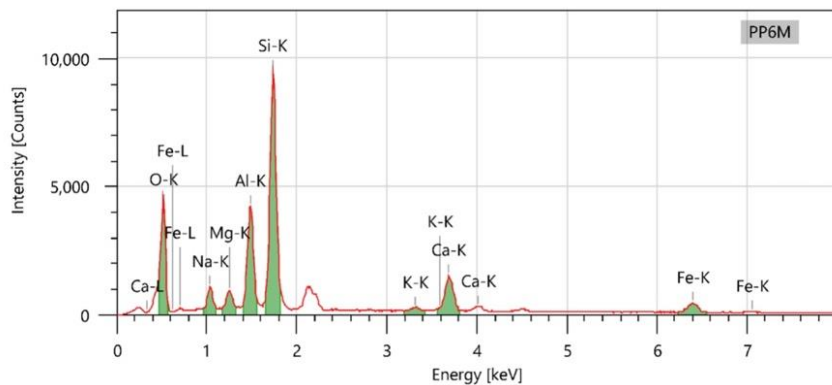
RESULT AND DISCUSSION

Mineral Content by EDX

EDX is used for the characterization of the mineral content of silica. The secondary electron source in EDX will hit the sample and the detector in EDX will capture the maximum intensity in each sample [29], [30]. The spectrum of EDX analysis results is shown in Figure 3.



(a)



(b)

Figure 3. EDX Analysis Spectra of Nanosilica Sample Content Based on (a) Coastal and (b) River.

EDX can be used to qualitatively and quantitatively analyze. Quantitatively analyzes the percentage of each element [31]. The mineral content of nano-silica analyzed using EDX is shown in Table 1.

Table 1. Mineral Content of Synthesized Nanosilica

Element	Atomic percentage (%)
---------	-----------------------

	Nanosilica based on River sand	Nanosilica based on Coastal Sand
O	58.64±0.55	47.51±0.85
Na	3.57±0.09	3.76±0.16
Fe	1.90±0.08	3.96±0.18
Ca	3.76±0.08	5.77±0.15
Si	19.35±0.17	25.63±0.31
K	0.39±0.02	0.46±0.04
Al	10.34±0.12	10.73±0.20
Ti	0.70±0.04	-
Mg	1.35±0.05	2.18±0.10

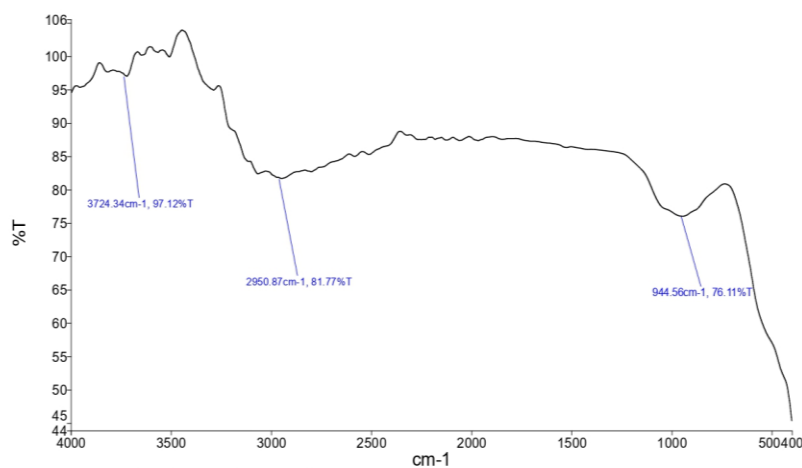
Table 1 shows the mineral content of nano-silica analyzed by using EDX. Table 1 shows that the largest mineral content based on coastal and river sand is silica. Where there is (19.35 ± 0.17) % in river sand-based silica and (25.63 ± 0.31) % in coastal-based silica. However, no titanium content was found in the nano-silica based on coastal sand. This indicates that the impurities of nanosilica based on coastal sand are less than nanosilica based on river sand [32].

FTIR Analysis

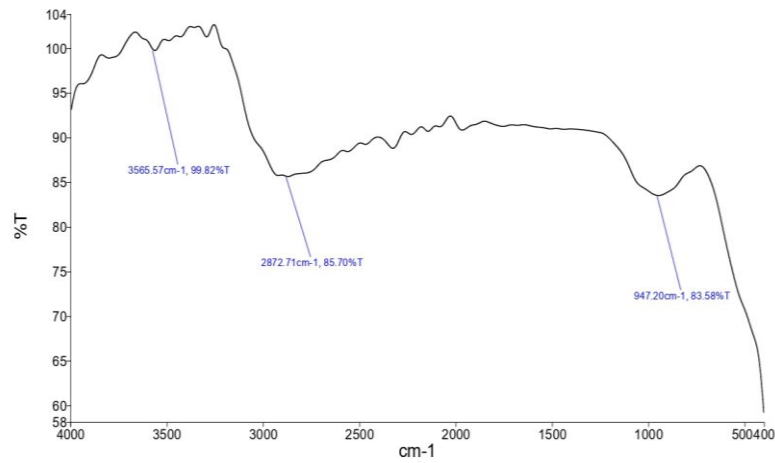
FTIR (Fourier Transform Infrared), is a modern infrared spectroscopy method equipped with Fourier transform techniques for detection and analysis of spectrum results [33]. The absorption spectrum as analyzed result of FTIR is shown in Figure 4.

Figure 4 shows wave absorption spectra from FTIR analysis of nano-silica based on (a) coastal and (b) river sand. The standard used is ASTM E1252. The mid-infrared region is the 400-4000 cm⁻¹ wavenumbers. Unlike EDX, which determines the percentage of mineral content using secondary electrons fired from a source, FTIR uses molecular vibrational wavelength analysis to determine the functional groups of a material [34], [35]. The functional group of nano-silica as FTIR analysis is shown in Table 2.

Table 2 shows the functional groups of nano-silica at specific absorption wavelengths. It appears that both coastal sand and river sand-based nano-silica have almost all absorption wavelengths with the same functional groups. Both river sand and coastal sand-based nano-silica have three functional groups namely OH group stretch vibrations in H₂O and Si-OH, Si-O stretch vibration of Si-O-Si (siloxane), Si-O asymmetric stretch vibration of silanol (Si-OH) [36], [37].



(a)



(b)

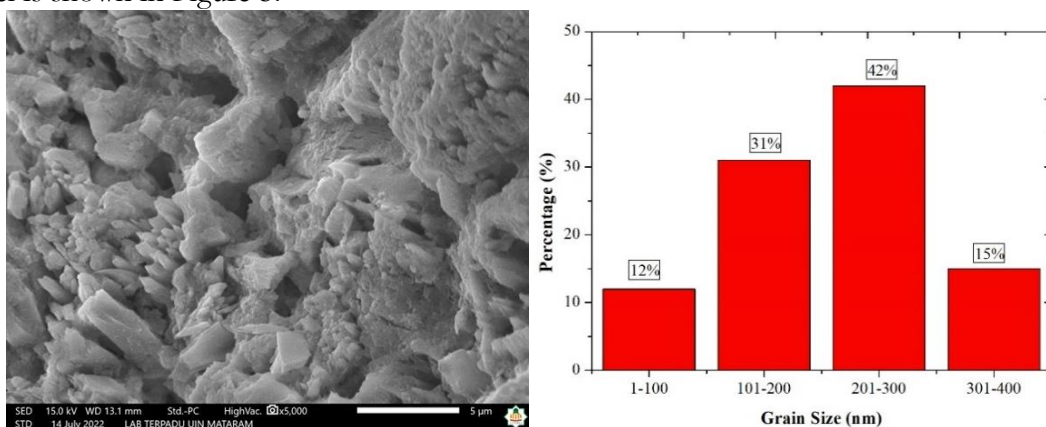
Figure 4. Wave Absorption Spectra From FTIR Analysis of Nanosilica Based on (a) Coastal Sand and (b) River Sand.

Table 2. Absorption Wavelengths of FTIR results.

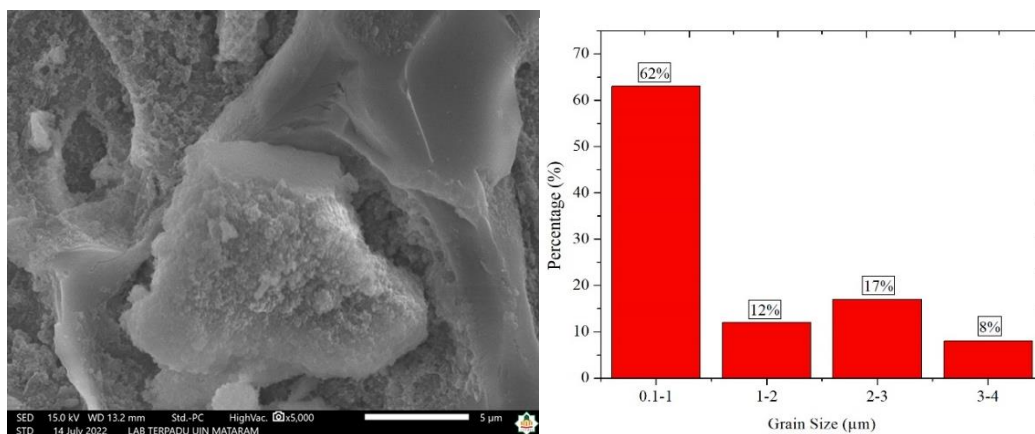
Nanosilica source	Wavelength absorption (cm-1)	Functional Group
Coastal sand	3724.34	OH group stretch vibrations in Si-OH and H ₂ O
	2950.87	Si-O stretch vibration of siloxane (Si-O-Si)
	944.56	Si-O asymmetric stretch vibration of silanol (Si-OH)
River sand	3565.57	OH group stretch vibrations in Si-OH and H ₂ O
	2872.71	Si-O stretch vibration of siloxane (Si-O-Si)
	947.20	Si-O asymmetric stretch vibration of silanol (Si-OH)

Morphological Characteristics

The morphology and grain size distribution of nano-silica were analyzed using a scanning electron microscope. Grain size is one of the most important physical properties because it can affect the general physical properties of materials such as optical properties, electrical properties, mechanical properties and magnetic properties [38], [39]. The morphology and grain size distribution of nano-silica gel is shown in Figure 5.



(a)



(b)

Figure 5. Morphology and Grain Size Distribution of Nanosilica Analyzed Using SEM (a) Coastal Sand and (b) River Sand.

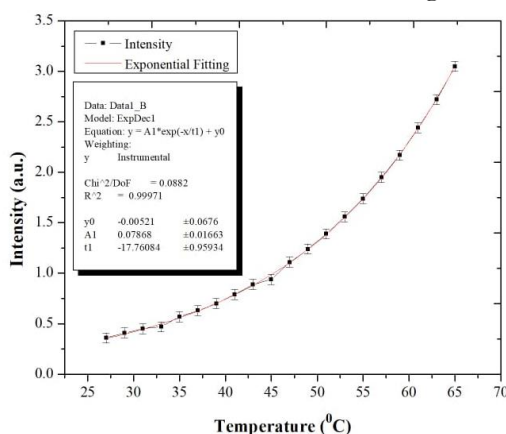
Figure 5 shows the morphology and grain size distribution of nano-silica analyzed using SEM. It appears that the nano-silica synthesized from coastal sand and river sand has a grain-shaped morphology. The coastal-based nanosilica has an average grain size of 359.47 nm which is much smaller than the river sand of 892.73 nm. Coastal sand has a much finer size than river sand. This is because coastal sand sediments are formed due to sea wave energy so that they have a finer structure. While river sand comes from limestone deposits that have fine and coarse structures [31].

SEM uses electron beams to image the surface shape of the sample being analyzed. SEM has a higher resolution than an optical microscope (OM). This is due to the de Broglie wavelength which has shorter electrons than the OM wave. Because the smaller the wavelength used, the higher the resolution of the microscope. SEM has a higher resolution than OM. The resolution that OM can produce is only 200 nm, while the resolution that SEM can produce reaches 0.1 - 0.2 nm [39], [40].

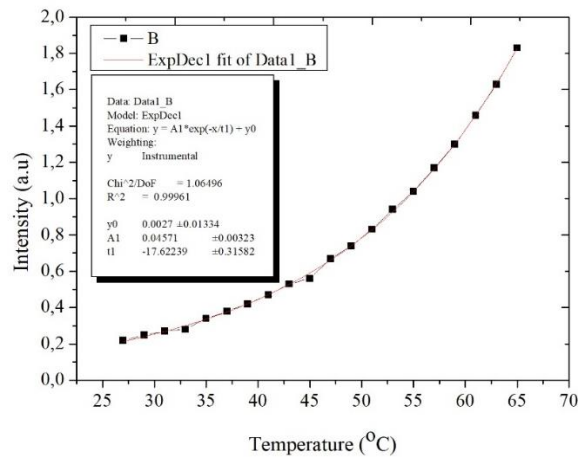
There are several important signals generated by the SEM. From the inelastic reflection, the secondary electron signal and X-ray characteristics are obtained, while from the elastic reflection, the backscattered electron signal is obtained [40], [41]. The differences between the images of secondary and backscattered electron signals are as follows: Secondary electrons produce the topography of the analyzed object, and high surfaces are brighter in colour than low surfaces [36].

Temperature sensor characteristics of nano-silica

The nano-silica passed by the laser is very sensitive even at relatively small temperatures. When measurements were taken, the digital thermometer showed room temperature as the initial temperature. It appears that at about 35°C, the intensity on the lux meter starts to increase due to the thermal effect. The results for laser intensity transmission as a function of temperature for the increasing temperature without an external field are shown in Figure 6.



(a)



(b)

Figure 6. Graph Of Nanosilica Gel Response to Temperature (a) on Coastal Sand (b) River Sand

Figure 6 shows silica an impact on increasing the magnetic properties of the nano-silica agglomeration process due to thermal agitation and increasing the optical properties of magnetite which accelerates the transmittance process of the applied laser. The equation obtained after fitting results for nano-silica based on coastal and river sand is shown in Equation 1.

$$y = y_0 + A \exp\left(-\frac{x}{R}\right) \tag{1}$$

Where y is the intensity, x is the temperature, y0 is -0.00521, A is 0.07868, R0 is 0.05691 on the sand coastal and y0 is 0.0027, A is 0.04571, R0 is =17.62239 indicating that the intensity of the laser beam imposed on the nano-silica sample will be proportional to the exponential change in temperature by the theory.

Based on Figure 6, it can be seen that when the laser is passed through the silica without the influence of the external field, the maximum intensity achieved is about 3.5 lux with a maximum temperature of 65 °C. The intensity is initially 0.4 lux, as the temperature increases, the intensity value also increases with a relatively small temperature change [21].

Since thermal agitation can suppress the ability of agglomeration, optical transmission can be regulated by changing the ambient temperature around the nano-silica [42]. Thus, this preliminary study opens a great opportunity for the synthesized nano-silica to be applied as a temperature sensor, especially based on iron sand mineral magnetic.

CONCLUSION

Based on data analysis, it is obtained that nano-silica based on coastal sand has a greater silica than nanosilica based on river sand. The morphology of nanosilica based on coastal sand is granular with a smaller grain size compared to river sand. Concerning a temperature sensor, nano-silica based on coastal sand has a larger coefficient when compared to nanosilica based on river sand. This indicates that nano-silica based on coastal sand has better physical properties as a temperature sensor than nanosilica based on river sand.

ACKNOWLEDGE

We would like to thank Kementerian Agama Republic Indonesia for the BOPTN research fund at Lembaga Penelitian dan Pengabdian kepada Masyarakat of Universitas Islam Negeri Mataram in 2022.

REFERENCES

- [1] L. A. D. Meiliyadi, M. Wahyudi, I. Damayanti, and A. Fudholi, “Morphological characteristics and electrical properties analysis of silica based on river and coastal iron sand,” *J. Ilm. Pendidik. Fis. Al-Biruni*, vol. 11, no. 1, pp. 129–140, 2022, doi: 10.24042/jipfalbiruni.v11i1.12390.

- [2] F. Ningsih, Fitrianiingsih, and L. A. Didik, "Analisis Pengaruh Lama Penggerusan terhadap Resistivitas dan Konstanta Dielektrik pada Pasir Besi yang disintesis dari Kabupaten Bima," *Indones. Phys. Rev.*, vol. 2, no. 3, pp. 92–98, 2019, doi: 10.29303/ipr.v2i3.31.
- [3] C. M. Marik *et al.*, "The efficacy of zero valent iron-sand filtration on the reduction of Escherichia coli and Listeria monocytogenes in surface water for use in irrigation," *Environ. Res.*, vol. 173, no. February, pp. 33–39, 2019, doi: 10.1016/j.envres.2019.02.028.
- [4] B. Satria, Z. M. Silvia, and J. Fajar, "Magnetic susceptibility and grain size distribution as prospective tools for selective exploration and provenance study of iron sand deposits: A case study from Aceh, Indonesia," *Heliyon*, vol. 7, p. e08584, 2021, doi: 10.1016/j.heliyon.2021.e08584.
- [5] L. A. D. Meiliyadi, M. Wahyudi, K. Arizona, and Z. A. Zain, "Synthesis of Nanosilica Gel Based on River Sand and Its Use as Water Treatment," *J. Mater. Environ. Sci.*, vol. 14, no. 11, pp. 1204–1213, 2023.
- [6] L. A. Didik and M. Wahyudi, "Analisa Kandungan Fe dan Karakteristik Sifat Listrik Pasir Besi Pantai Telindung yang Disintesis Dengan Beberapa Metode," *Indones. Phys. Rev.*, vol. 3, no. 2, pp. 64–71, 2020, doi: 10.29303/i pr.v3i2.58.
- [7] R. Gannoun, J. M. P. Ebrí, A. T. Pérez, M. J. Espín, F. J. Durán-Olivencia, and J. M. Valverde, "Nanosilica to improve the flowability of fine limestone powders in thermochemical storage units," *Chem. Eng. J.*, vol. 426, p. 131789, 2021, doi: 10.1016/j.cej.2021.131789.
- [8] G. Fan, M. Li, X. Chen, A. Palyanitsina, and A. Timoshin, "Polymer-Nanosilica-assisted to evaluate oil recovery performances in sandstone reservoirs," *Energy Reports*, vol. 7, pp. 2588–2593, 2021, doi: 10.1016/j.egyr.2021.04.047.
- [9] S. Azizi and N. Shadjou, "Iron oxide (Fe₃O₄) magnetic nanoparticles supported on wrinkled fibrous nanosilica (WFNS) functionalized by biimidazole ionic liquid as an effective and reusable heterogeneous magnetic nanocatalyst for the efficient synthesis of N-sulfonylamidines," *Heliyon*, vol. 7, p. e05915, 2021, doi: 10.1016/j.heliyon.2021.e05915.
- [10] Z. Xantini and E. Erasmus, "Platinum supported on nanosilica and fibrous nanosilica for hydrogenation reactions," *Polyhedron*, vol. 193, p. 114769, 2021, doi: 10.1016/j.poly.2020.114769.
- [11] P. Dileep, S. Jacob, and S. K. Narayanankutty, "Functionalized nanosilica as an antimicrobial additive for waterborne paints," *Prog. Org. Coatings*, vol. 142, p. 105574, 2020, doi: 10.1016/j.porgcoat.2020.105574.
- [12] Fernández-Fernández, Á. C. M., and M. M., "Molecular simulation of methane hydrate growth confined into a silica pore," *J. Mol. Liq.*, vol. 362, p. 119698, 2022, doi: 10.1016/j.molliq.2022.119698.
- [13] Y. Liu, J. Liu, Z. Wang, Y. Yuan, J. Hua, and K. Liu, "Robust and durable superhydrophobic and oil-absorbent silica particles with ultrahigh separation efficiency and recyclability," *Microporous Mesoporous Mater.*, vol. 335, p. 111772, 2022, doi: 10.1016/j.micromeso.2022.111772.
- [14] K. Luo *et al.*, "Hydrophobic and hydrophilic selectivity of a multifunctional carbonyldiimidazolium/dodecyl modified silica stationary phase," *J. Chromatogr. A*, vol. 1677, p. 463300, 2022, doi: 10.1016/j.chroma.2022.463300.
- [15] Y. Cheng and L. Zheng, "Engineering silica encapsulated composite of acyltransferase from Mycobacterium smegmatis and MIL-88A: A stability-and activity-improved biocatalyst for N-acylation reactions in water," *Colloids Surfaces B Biointerfaces*, vol. 217, p. 112690, 2022, doi: 10.1016/j.colsurfb.2022.112690.
- [16] Z. Dong, X. Jin, and G. Zhao, "Amplified QCM biosensor for type IV collagenase based on collagenase-cleavage of gold nanoparticles functionalized peptide," *Biosens. Bioelectron.*, vol. 106,

- no. November 2017, pp. 111–116, 2018, doi: 10.1016/j.bios.2018.01.069.
- [17] F. Zhao *et al.*, “Energy storage performance of silicon-integrated epitaxial lead-free BaTiO₃-based capacitor,” *Chem. Eng. J.*, vol. 450, no. 3, p. 138312, 2022, doi: 10.1016/j.cej.2022.138312.
- [18] P. Pal, H. Li, and S. Saravanamurugan, “Removal of lignin and silica from rice straw for enhanced accessibility of holocellulose for the production of high-value chemicals,” *Bioresour. Technol.*, vol. 361, p. 127661, 2022, doi: 10.1016/j.biortech.2022.127661.
- [19] K. Vopel, C. Pook, P. Wilson, and J. Robertson, “Offshore iron sand extraction in New Zealand: Potential trace metal exposure of benthic and pelagic biota,” *Mar. Pollut. Bull.*, vol. 123, no. 1–2, pp. 324–328, 2017, doi: 10.1016/j.marpolbul.2017.09.018.
- [20] L. A. Didik, Yahdi, and Masrurroh, “Improvement QCM Quality by Polystyrene Coating and Bovine Serum Albumin as Immobilization Agent,” *Al-Biruni*, vol. 08, no. 1, pp. 35–41, 2019, doi: 10.24042/jipfalbiruni.v8i1.3716.
- [21] V. Kumar, R. Adalati, Y. K. Gautam, and D. Gautam, “An investigation of glass, ITO, and quartz transparent substrates on Pd/SnO₂ hydrogen sensor structure and sensitivity,” *Mater. Today Commun.*, vol. 5, p. 109280, 2024, doi: 10.1016/j.mtcomm.2024.109280.
- [22] F. N. Dultsev and D. V. Nekrasov, “Treatment of the resonance curve recorded during measurement of the signal of particle rupture from the QCM surface,” *Sensors Actuators B. Chem.*, 2018, doi: 10.1016/j.snb.2018.04.029.
- [23] H. Kiyomoto, Y. Sakai, and Y. Kansha, “Evaluation of isothermal and isofield designs of a temperature sensor using magnetic phase transition,” *Therm. Sci. Eng. Prog.*, vol. 50, p. 102597, 2024, doi: 10.1016/j.tsep.2024.102597.
- [24] J. Ban *et al.*, “Highly sensitive stretchable fiber-based temperature sensor enhanced by surface-chemically modified silver nanowires,” *Chem. Eng. J.*, vol. 482, p. 148772, 2024, doi: 10.1016/j.cej.2024.148772.
- [25] W. C. Zheng, D. X. Zheng, Y. C. Wang, D. Li, C. Jin, and H. L. Bai, “Flexible Fe₃O₄/BiFeO₃ multiferroic heterostructures with uniaxial strain control of exchange bias,” *J. Magn. Magn. Mater.*, vol. 481, pp. 227–233, 2019, doi: 10.1016/j.jmmm.2019.02.068.
- [26] A. Ananda and S. Aini, “Sintesis Silika Mesopori Menggunakan Bahan Dasar Na₂SiO₃ yang Dihasilkan dari Pasir Silika dengan Metoda Sol-Gel,” *Periodic*, vol. 10, no. 1, pp. 37–39, 2021, doi: 10.24036/p.v10i1.110482.
- [27] Bramantya, L. P. Yonando, M. Rifaldi, and R. Oktavian, “Sintesis dan Karakterisasi Silika Aerogel Hidrofobik dan Olioofilik Dari Pasir Laut Sebagai Absorben Tumpahan Minyak,” *J. Tek. Kim. dan Lingkungan*, vol. 2, no. 2, pp. 49–54, 2018, doi: 10.25077/jfu.10.3.296-302.2021.
- [28] K. D. Gautam and A. V. Ullas, “Effect of Stirring Speed on the Morphology of Nanosilica by Sol-Gel method,” *Mater. Today Proc.*, vol. 74, no. 4, pp. 713–717, 2023, doi: 10.1016/j.matpr.2022.10.281.
- [29] M. A. Zayed, N. G. Imam, M. A. Ahmed, and D. H. El Sherbiny, “Spectrophotometric analysis of hematite/magnetite nanocomposites in comparison with EDX and XRF techniques,” *J. Mol. Liq.*, vol. 211, pp. 288–295, 2017, doi: <http://dx.doi.org/10.1016/j.molliq.2017.02.007>.
- [30] M. R. Fahlepy, V. A. Tiwow, and Subaer, “Characterization of magnetite (Fe₃O₄) minerals from natural iron sand of Bonto Kanang Village Takalar for ink powder (toner) application,” *J. Phys. Conf. Ser.*, vol. 997, no. 1, 2018, doi: 10.1088/1742-6596/997/1/012036.
- [31] L. A. Didik, I. Damayanti, J. Jumliati, and P. D. Alfadia Lestari, “Morphological Characteristics and Mineral Content Analysis of Magnetic Minerals Based on River and Coastal Sand using SEM-EDX,” *J. Sains Dasar*, vol. 10, no. 2, pp. 44–50, 2021, doi: 10.21831/jsd.v10i2.42217.
- [32] E. Sukirman, Y. Sarwanto, A. Insani, M. Th. Rina, and A. Purwanto, “Magnetic Structure of

- Magnetite Phase of Iron Sand Retrieved from Banten, Indonesia,” *J. Phys. Conf. Ser.*, vol. 1091, no. 1, 2018, doi: 10.1088/1742-6596/1091/1/012007.
- [33] F. Malega, I. P. T. Indrayana, and E. Suharyadi, “Synthesis and Characterization of the Microstructure and Functional Group Bond of Fe₃O₄ Nanoparticles from Natural Iron Sand in Tobelo North Halmahera,” *J. Ilm. Pendidik. Fis. Al-Biruni*, vol. 7, no. 2, p. 129, 2018, doi: 10.24042/jipfalbiruni.v7i2.2913.
- [34] P. Sebayang *et al.*, “Preparation of Fe₃O₄/Bentonite Nanocomposite from Natural Iron Sand by Co-precipitation Method for Adsorbents Materials,” *IOP Conf. Ser. Mater. Sci. Eng.*, vol. 316, no. 1, 2018, doi: 10.1088/1757-899X/316/1/012053.
- [35] C. Kurniawan *et al.*, “Synthesis and Characterization of Magnetic Elastomer based PEG-Coated Fe₃O₄ from Natural Iron Sand,” *IOP Conf. Ser. Mater. Sci. Eng.*, vol. 202, no. 1, 2017, doi: 10.1088/1757-899X/202/1/012051.
- [36] S. Sumari, M. R. Asrori, Y. F. Prakasa, D. R. Baharintasari, and A. Santoso, “Silica extract from Malang beach sand via leaching and sol-gel methods,” *Int. J. Adv. Appl. Sci.*, vol. 12, no. 1, p. 74, 2023, doi: 10.11591/ijaas.v12.i1.pp74-81.
- [37] N. M. Tran, Y. Nam, and H. Yoo, “Fabrication of dendritic fibrous silica nanolayer on optimized water-glass-based synthetic nanosilica from rice husk ash,” *Ceram. Int.*, vol. 48, no. 21, pp. 32409–32417, 2022, doi: 10.1016/j.ceramint.2022.07.184.
- [38] L. A. Didik and Muh. Wahyudi, “Crystal Structure Analysis of CuCrO₂ Based On XRD Data Using GSAS Software,” *Indones. Phys. Rev.*, vol. 4, no. 1, pp. 10–17, 2021, doi: <https://doi.org/10.29303/ipr.v4i1.73>.
- [39] L. A. Didik, E. Rahmawati, F. Robiandi, S. Rahayu, and D. J. D. H. Santjojo, “Penentuan Ketebalan Lapisan Polistiren dan Zinc Phthalocyanine (ZnPc) dengan Modifikasi Persamaan Sauerbrey dan Scanning Electron Microscope (SEM),” *Nat. B*, vol. 2, no. 4, pp. 331–335, 2014, doi: 10.21776/ub.natural-b.2014.002.04.6.
- [40] E. A. Setiadi *et al.*, “The effect of temperature on synthesis of MgFe₂O₄ based on natural iron sand by Co-precipitation method as adsorbent Pb ion,” *J. Phys. Conf. Ser.*, vol. 985, no. 1, 2018, doi: 10.1088/1742-6596/985/1/012046.
- [41] M. Rianna *et al.*, “Characterization of Natural Iron Sand From Kata Beach, West Sumatra With High Energy Milling (Hem),” *J. Nat.*, vol. 18, no. 2, pp. 97–100, 2018, doi: 10.24815/jn.v18i2.11163.
- [42] W. Elyani, A. Hidayat, A. Taufiq, and Sunaryono, “Sintesis Kromium Ferit dari Pasir Pantai dan Karakterisasi Awal Sensor Suhu,” *JPSE (Journal Phys. Sci. Eng.)*, vol. 3, no. 1, pp. 1–7, 2018, doi: 10.17977/um024v3i12018p001.